

## **Estimation of Charge Carrier Density of Turmeric Dye in the Presence of Polyvinyl Alcohol (PVA) and Its Electrical Characterization as Herbal Diode**

**S. Bhunia<sup>1\*</sup>, P. K. Das<sup>2</sup>, S. Rakshit<sup>3</sup>, N. B. Manik<sup>3</sup>**

<sup>1</sup>Department of Physics, Ramakrishna Residential College, Narendrapur, Kolkata-700103, India

<sup>2</sup>Department of Electronics, Behala College, Behala, Kolkata-60, India

<sup>3</sup>Condensed Matter Physics Research Centre, Department of Physics, Jadavpur University, Kolkata-700032, India

Received 3 February 2021, accepted in final revised form 10 September 2021

### **Abstract**

The study on the semiconducting properties of herbal dye and various parameters of the herbal dye-based device is an important area of research in the coming days. In this work, we have measured the conductivity and Hall coefficient of turmeric dye in solid thin film form. Using the working principle of the Hall Effect, we have measured the Hall coefficient (HC) of this film. It is found that the curves of Hall voltage ( $V_H$ ) – Hall current ( $I_C$ ) and Hall voltage ( $V_H$ ) – Magnetic field ( $B_H$ ) are linear. The Hall coefficient has been estimated from these curves. The average value of the Hall coefficient (R) is  $22.64 \times 10^{-4} \text{ m}^3/\text{C}$ . The conductivity ( $\sigma$ ) of the film is  $1.5 \times 10^{-10} \Omega \text{ m}^{-1}$ . We have estimated charge carrier density from this parameter, and its typical value is  $2.8 \times 10^{23} \text{ m}^{-3}$ . We have also prepared a diode using this turmeric dye and extracted reverse saturation current, rectification ratio, ideality factor, series resistance, etc. It has been noticed that the diode exhibits high ideality factor and series resistance. The presence of traps is one of the main reasons for these high values. So, we have also measured the trapped energy of the device considering exponential trap distribution.

**Keywords:** PVA turmeric composite film; Hall coefficient; Carrier concentration; Ideality factor; Series resistance.

© 2022 JSR Publications. ISSN: 2070-0237 (Print); 2070-0245 (Online). All rights reserved.

doi: <http://dx.doi.org/10.3329/jsr.v14i1.51841>

J. Sci. Res. **14** (1), 11-25 (2022)

### **1. Introduction**

The study of different herbal dyes and their applications in the vast area is the new era of science. Earlier, herbal dyes are used for coloring food substrate, leather, and fibers like wool, silk, and cotton [1,2]. Herbal dyes also have a significant impact on Ayurveda medicine. The presence of anticancer properties in herbal dyes has also been observed by few researchers. Now a day herbal dyes are used as the color and flavor of the diet. They are also used in electronic and optoelectronic devices due to the conducting nature of herbal dyes [3-6]. Recently different herbal dyes are being studied to develop different

---

\* Corresponding author: [swapanbhunia1976@gmail.com](mailto:swapanbhunia1976@gmail.com)

electronic devices. These herbal dye-based devices have many advantages. The herbal dye-based devices are nature-friendly, biodegradable, and cost-effective. There are also varieties of dyes to study. It may be fabricated over a large area on different substrates from its solution by simple processing techniques, such as sol-gel, spin-coating, solvent casting, sublimation, dip coating, etc. [7-9]. Natural dyes like turmeric, Hibiscus Rosasinesis, and Sesbania Grandiflora are used as photosensitizers due to their large absorption coefficient in the visible region in the dye-sensitized solar cell [3,5]. One of the most important parameters in any electronic device is the amount of charge carrier density, which controls the overall device performance. So, it will be essential to obtain the charge carrier density, ideality factor, and series resistance to better understand and improve the herbal dye-based devices.

As the herbal materials are disordered amorphous solids and dominated by weak van der Waals forces, there is no definite band structure. The highest occupied molecular orbital (HOMO) and lowest unoccupied molecular orbital (LUMO) are represented the band structure instead of the valence band and conduction band. Therefore, the charge carriers in the charge conduction process in the herbal dye-based devices are mainly free electrons and holes generated from the  $\pi$  orbitals. Also, during the charge transport process, these charges are traveling from one molecule to another and depend on the energy gap between HOMO and LUMO. Nevertheless, some works reported on the performance and electrical characterization of the herbal dye-based devices [10,11], but the study on the charge carrier density of the herbal dye-based devices has not been properly discussed.

Moreover, it is also observed from the earlier works that the overall performance of the herbal dye-based devices is very poor [12]. One of the important reasons for the degradation of performance is the band structure of the herbal dye that influences the charge injection and the flow of charge carriers in the herbal dye-based devices. Another reason is trap distribution in the energy space between HOMO and LUMO in the herbal material [13-15]. These traps are again two types one is shallow traps, and another one is deep traps, which result in different unusual anomalous properties in electrical characteristics. These traps decrease the device performance. So, it will be essential to know about the charge carrier density and the conductivity of the herbal dye-based devices.

So, in this work, we have studied the magnetic field effect and estimated charge carrier density of the herbal dye-based device. For this study, we have chosen turmeric dye [ $C_{21}H_{20}O_8$ ] as the active material. Among the other herbal dyes, turmeric is easily available and the cheapest natural dye. It is nothing but a powder form of rhizome of a natural plant named Curcuma Longa L [16]. Here we have assumed the current carriers present in the device due to the breaking of  $\pi^*$  bond. The magnetic force on the carrier [17] is

$$E_m = e(v \times H) \quad (1)$$

And it is compensated by Hall field ( $F_h$ )

$$F_h = e E_h \quad (2)$$

Where  $\mathbf{v}$  is drift velocity of the carrier.

$$\text{So } E_h = R\mathbf{J} \times \mathbf{H} \tag{3}$$

Where current density ( $\mathbf{J}$ ) =  $qn\mathbf{v}$

From Eqs. (1), (2) and (3) we can write

$$\mathbf{R} = \frac{V_h \mathbf{Z}}{JH}$$

Where  $V_h$  is Hall voltage, as  $J$  is along the X direction,  $H$  is along Z direction, so  $E_h$  will be along Y direction. For one type of carrier, I can write

$$\text{Hall coefficient (R)} = \frac{E_h}{JH} = \frac{vH}{qnvH} = \frac{1}{nq} \tag{4}$$

From experiments in modern physics by Adrian C. we can say for two types carrier Hall Co-efficient will be [6]

$$R = \frac{\mu_p^2 p - \mu_e^2 n}{2(\mu_p - \mu_e)^2} \tag{5}$$

Where mobility of holes and electrons are defined by  $\mu_p$  and  $\mu_e$ , and the carrier densities of holes and electrons are represented by  $p$  and  $e$ . Here we assume the carrier is an electron due to breaking  $\pi^*$  bond. We choose  $\mu_p$  is zero. So, Eq. (5) reduces Eq. (4). Hall voltage is proportional to  $1/n$  or its resistivity when the magnetic field and input current are fixed. In this system, one carrier dominates

So, conductivity  $\sigma = n q \mu$  where  $\mu$  is the mobility of charge carriers.

$$\text{Thus } \mu = R \sigma \text{ here } \sigma = 1.5 \times 10^{-10} \text{ } \Omega^{-1} \text{ m}^{-1}$$

Apart from that, after observing the conductivity and charge carrier density, we have also prepared one turmeric dye-based diode. Various important parameters such as rectification ratio, ideality factor, series resistance, and reverse saturation current, etc., of the device have been extracted. To prepare the diode, we have sandwiched the turmeric herbal dye in between two electrodes; one is ITO which acts as a front electrode, and another is Al, which acts as a back electrode. The chemical composition of turmeric dye has shown in Fig. 1. The melting point is 183 °C. To measure various important parameters of the diode, we have analyzed the dark IV characteristics by using the Shockley equation given below [18].

$$I = I_0 \left[ \exp\left(\frac{qV}{nkT}\right) - 1 \right] \tag{6}$$

Where  $I_0$  is the reverse saturation current which is given by,

$$I_0 = AA^* T^2 \exp\left(-\frac{q\phi}{kT}\right) \tag{7}$$

Where  $I_0$  is the reverse saturation current,  $q$  is the electronic charge,  $K$  is the Boltzmann constant,  $T$  is the temperature,  $V$  is the applied voltage,  $n$  is the ideality factor.

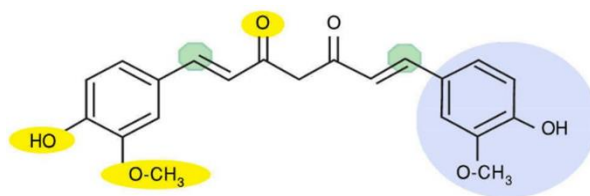


Fig. 1. Structure of Curcumin.

## 2. Measurement

### 2.1. Estimation of charge carrier density

In this work to estimate the charge carrier density of turmeric dye-based thin film, we had performed the Hall experiment method. At first, we prepared a Hall sample. Then two clean glass plates of  $3 \times 2 \text{ cm}^2$  and four adhesive Cu tape of length 1.5 cm were taken. These two glass plates were cleaned with distilled water and acetone, and they were dried under vacuum ( $10^{-3} \text{ mm}$ ) for 3 h. Two Cu tapes were attached along the X-axis, keeping separation 1.5 cm. Another two are attached along the Y-axis, keeping separation 1 cm on a cleaned glass plate. To form a transparent viscous solution of polyvinyl alcohol 1 g of polyvinyl alcohol (PVA) was added in 15 mL of double-distilled water and stirred well. Here PVA acted as an inert binder. We have found that turmeric dye is in both the hydrophobic and hydrophilic pockets of PVA; aqueous PVA solution could be easily cross-linked to form a hydrogel and loaded with turmeric dye. It is well known that PVA is used in various applications due to its amazing properties, such as water-soluble nature, high optical transmission, and stable thermal properties. Apart from that PVA is flexible and possesses oxygen/aroma barrier properties. When PVA is mixed with some other semiconducting dye, an abundance of hydroxyl groups attached to its carbon backbone originates a big source of hydrogen bonding that has a major effect on its physicochemical bulk properties. Therefore, due to this hydrogen bonding between PVA chains, they exhibit binder properties. In this present work, we have used this turmeric dye as the active material of the device. With increasing dye concentration, we can enhance the charge carriers during the charge transport process, which will enhance the overall current of the device. Earlier few studies have been carried out on the effect of turmeric dye concentration on performance [19]. We have also observed that current is more for higher dye concentration. We took 5 mL PVA solution in a cleaned test tube and added 1 gm turmeric powder, which was purchased from FGO product. This mixture was stirred well by a magnetic stirrer. 2 mL of this semi-solid was then spin-coated on a special type of glass plate with motor speed 800 rpm (Fig. 2). A clean glass plate was placed on a turmeric dye-based special type of glass plate and bounded tightly by transparent cello tape. Now turmeric thin film was dried under vacuum ( $10^{-3} \text{ mm}$ ) for 10 h. Here another glass plate used for protection from surroundings. Now Hall sample was ready to measure the Hall coefficient. Model and a digital image of Hall sample have shown in Figs. 2a and

2b. respectively. The circuit diagram and digital image of the Hall setup have shown in Figs. 3a and 3b, respectively.

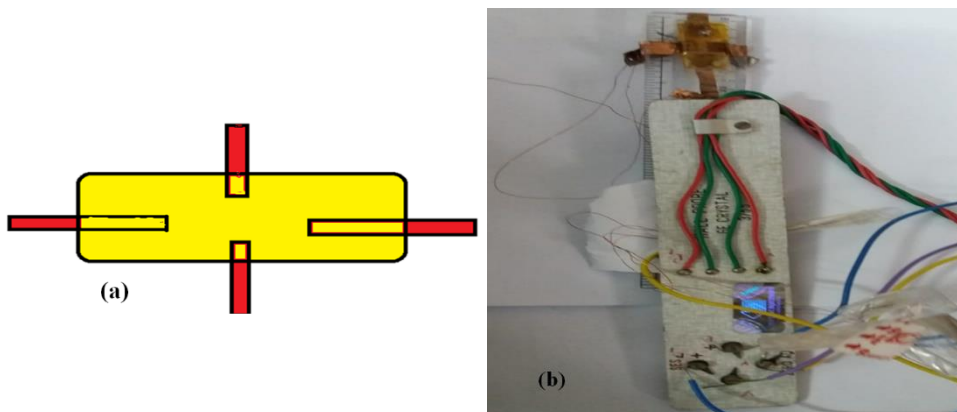
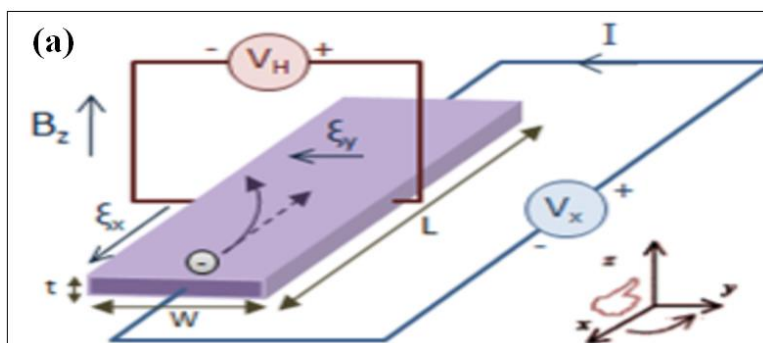


Fig. 2. (a) Special type of cell used for Hall experiment and (b) digital image of Hall probe.

We have prepared a turmeric dye-based Hall sample for the Hall experiment. We have connected the Hall sample with the Hall probe supplied Hall set up (Digital, DHE-21). The Hall probe has four terminals, two terminals are voltage connectors, and the other two are current connectors. Hall sample has four Cu tape; two are along X-axis and another two along Y-axis. We have connected voltage connector with X-axis Cu tape and current connector with Y-axis Cu tape. We have used Hall set up (Digital, DHE-21) and electromagnet model EMU-75. We have taken Digital Gaussmeter (DGM-102) and constant power supply (DPS-175) for magnetic field measurement. After setting "zero field potential" we have placed the Hall sample in the magnetic field according to Fig. 3, and we have switched on the electromagnet power supply and adjusted the current 2 mA. We have rotated the Hall sample till it becomes perpendicular to the magnetic field. Hall voltage will be maximum in this adjustment. We have measured Hall voltage for both directions of the current and magnetic field. We have measured the Hall voltage as a function of current keeping the magnetic field constant. Similarly, we have measured Hall voltage as a function of the magnetic field keeping current constant.



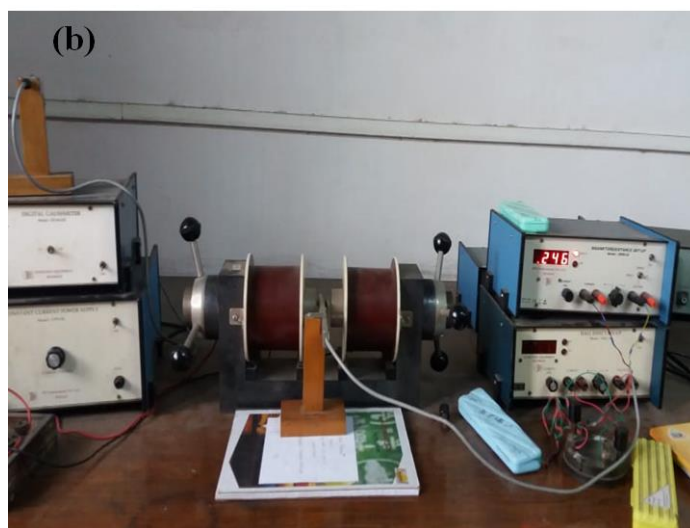


Fig. 3. (a) Hall probe connection setup and (b) digital image Hall set up.

## ***2.2. Study of the electrical characteristic of turmeric dye-based herbal diode***

To prepare the diode at first, we had mixed 1 mg PVA (purchased from S. D. Fine Chem. Ltd., Boisar, India) with 10 mL distilled water in a cleaned beaker and produced a PVA solution. Then the PVA solution was stirred for 30 min with a magnetic stirrer. After that, 20 mg turmeric dye was mixed with the prepared PVA solution and stirred the solution well for another 30 min to prepare the turmeric dye solution. Then at first, we had spin-coated the solution on ITO coated glass at a speed of 1500 rpm, which again dried at a speed of 2500 rpm. Then similarly, this solution was spin-coated on the Aluminium electrode and dried. After that, we had sandwiched these two electrodes together to form the turmeric dye-based herbal diode [20]. This prepared turmeric dye-based herbal diode was then kept in a vacuum for 12 h before the characterization [21]. Fig. 4 shows the schematic structure of the turmeric dye-based herbal diode.

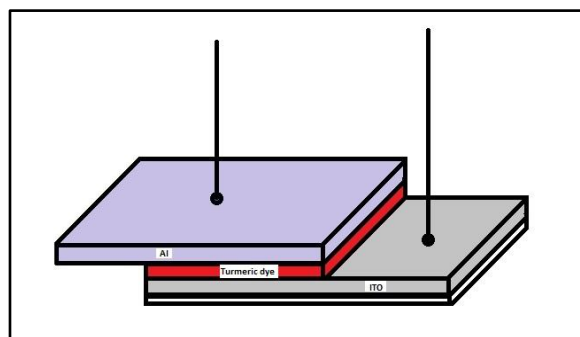


Fig. 4. Schematic diagram of turmeric dye-based organic device.

After preparing the turmeric dye-based herbal diode, we measured the steady-state I-V characteristics of the diode using the Keithley 2400 source measure unit. For the measurement, we connected the battery's positive terminal to the ITO, and the negative terminal of the battery was connected to the Al electrode. The voltage across the device has been varied from 0 to 8 V in steps of 0.5 V. The experiment has been performed at a normal room temperature of 26 °C [18].

### 3. Results and Discussion

We have measured Hall voltage with varying Hall current keeping fixed magnetic field and plot the curve Fig. 5. Next, we have recorded Hall Voltage varying with magnetic field keeping fixed Hall current and plot the curve Fig. 6. We assume that curves are linear. We have estimated the Hall coefficient from these curves.

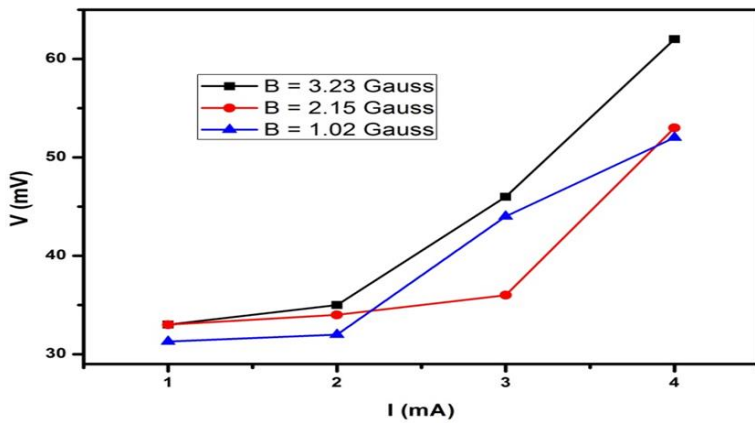


Fig. 5. I-V curve keeping fixed magnetic field.

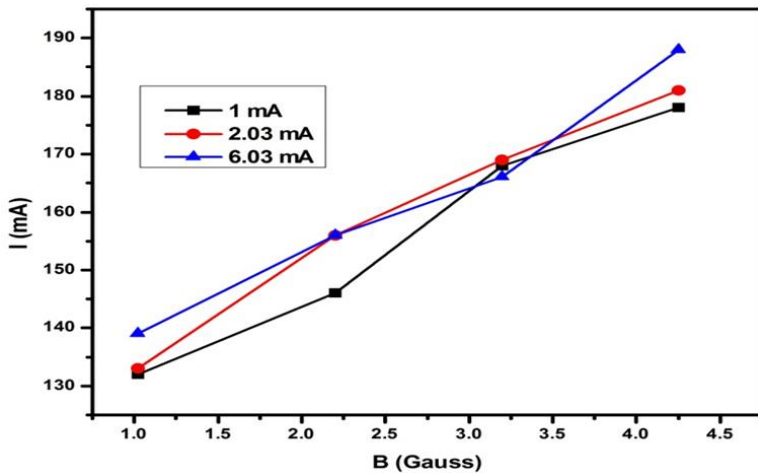


Fig. 6. I-B curve keeping fixed Hall current.

**Calculation of mobility and charge carrier density:**

Average Hall coefficient  $R = 0.0022 \text{ m}^3 \text{ Coulomb}^{-1}$

$$\text{Charge carrier density } n = \frac{1}{Rq} = 2.8 \times 10^{23} \text{ m}^{-3}$$

Mobility of charge carrier ( $\mu$ ) =  $R \sigma = 3.3 \times 10^{-13} \text{ m}^2 \text{ volt}^{-1} \text{ sec}^{-1}$

Table 1. Extracted value of Hall coefficient ( $R_H$ ) from  $B$  vs  $V_H$  and  $V_H$  vs  $I_H$  graphs.

Thickness of the sample in meter	$R_H$ from the slope of $B$ vs $V_H$ graph		$R_H$ from the slope of $V_H$ vs $I_H$ graph	
	Hall current $I$ in mA	$R_H = \frac{\Delta V_H Z}{\Delta B I}$ in $\text{m}^3 \cdot \text{Coulomb}^{-1}$	$B$ in Tesla	$R_H = \frac{\Delta V_H Z}{\Delta I B}$ in $\text{m}^3 \cdot \text{Coulomb}^{-1}$
$5 \times 10^{-4}$	2	$37.24 \times 10^{-4}$	0.050	$14.41 \times 10^{-4}$
	4.03	$18.34 \times 10^{-4}$	0.215	$29.20 \times 10^{-4}$
	6.02	$12.25 \times 10^{-4}$	0.323	$27.43 \times 10^{-4}$

We have estimated the Hall coefficient of turmeric dye film for different Hall currents shown in Table 1. Its values are different for different Hall currents. So, we have taken the average value Hall coefficient ( $R = 0.0022 \text{ m}^3 \text{ Coulomb}^{-1}$ ). We have calculated charge carrier density, and its value is ( $n = \frac{1}{Rq} =$ )  $2.8 \times 10^{23} \text{ m}^{-3}$ . We have compared the data with intrinsic Germanium (Ge), Silicon (Si), and Gallium Arsenide (GaAs). Charge carrier density in our device is more than Ge or Si. So, it is a breakthrough of herbal dye-based devices. As herbal dye-based devices are nature-friendly, biodegradable, and cost-effective, various electronic devices can be used.

In this work, we have also prepared one diode using this turmeric herbal dye and studied various parameters such as reverse saturation current, rectification ratio, ideality factor, and the diode series resistance. To study these parameters, we have observed the dark IV characteristics of this turmeric dye-based herbal diode. The dark IV characteristic of this diode has shown in Fig. 7.

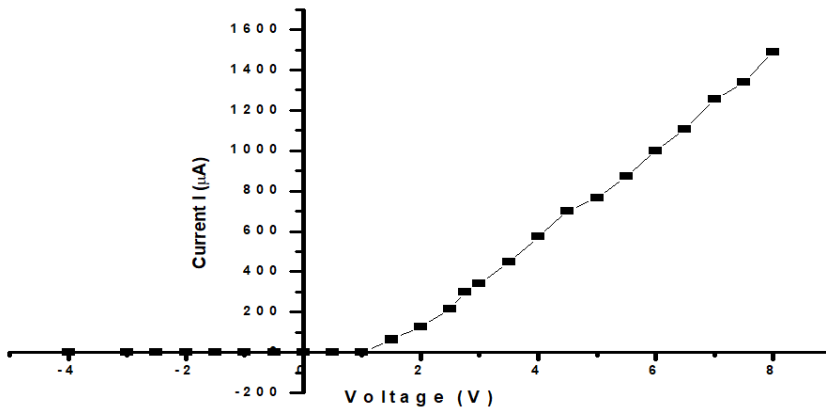


Fig. 7. dark I – V characteristic of ITO/turmeric/Al herbal diode.

From Fig. 7, it can be observed that the device exhibits diode-like behavior. It has also been observed that the value of the device current is very low, nearly in the microampere region. The rectification ratio of the device is 407 at 2.5 volts and has increased to 543 at 3.5 volts. Here, ITO is used as a high work function electrode. Al is used as a low work function electrode. Considering the turmeric dye as an n-type semiconductor, we have shown the band diagram of the ITO / turmeric dye/Al device in Fig. 8. This diagram shows that due to the difference in work functions of the electrodes, the ITO/ turmeric dye interface forms rectifying contact. In contrast, the Al/turmeric dye interface forms an ohmic contact.

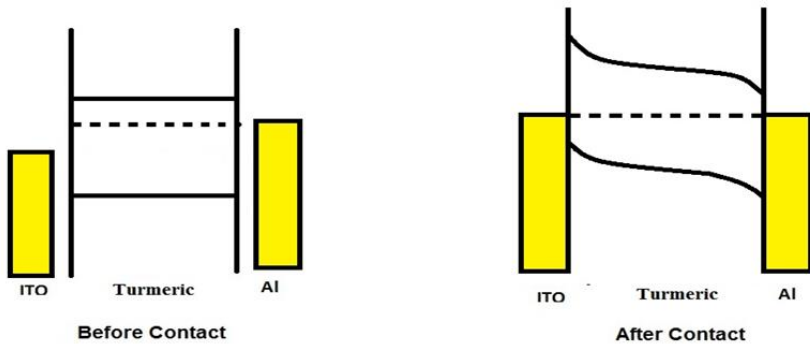


Fig. 8. Schematic energy band diagram of ITO/turmeric/Al interface where ITO/turmeric form Schottky contact and Al/turmeric form Ohmic contact.

So due to this rectifying contact, when we applied voltage across the device, the I-V characteristics of the device give an asymmetric curve.

The  $\ln I$  Vs.  $1/T$  plot of the turmeric dye-based herbal diode is shown in Fig. 9. From this figure, we have measured device reverse saturation current, which is nearly about 14.29  $\mu\text{A}$ . Also, we have measured the device ideality factor from the slope of the curve by using Eq. (8).

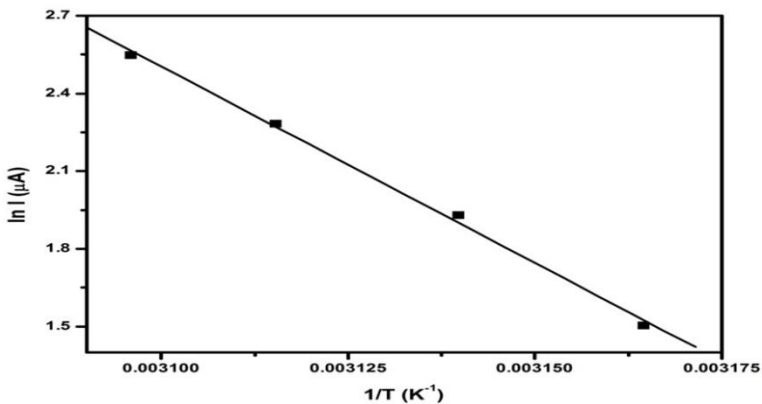


Fig. 9.  $\ln I$  versus  $1/T$  plot of turmeric dye-based herbal diode.

$$\eta = \frac{q}{kT} \frac{dV}{d \ln I} \tag{8}$$

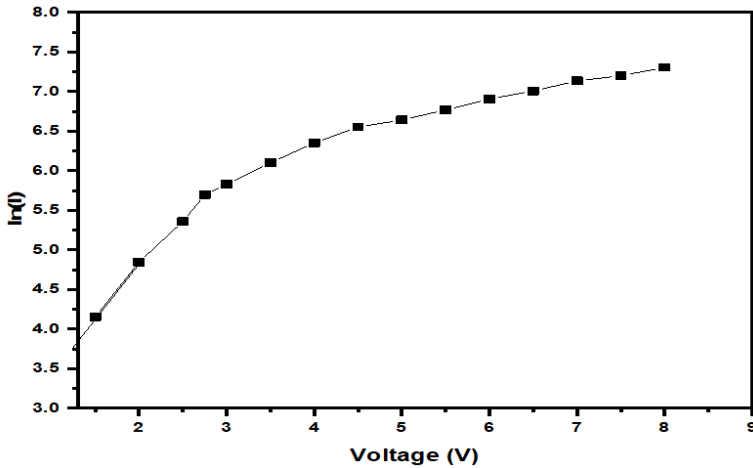


Fig. 10. lnI versus V plot of turmeric dye-based herbal diode.

The lnI Vs. V plot of the diode shows linearity at low voltage, but as the voltage increased, the curve deviates from its linearity Fig. 10. It is observed that the value of n is very high. The value of n of the diode is nearly about 18.84. The deviation of the curve occurred mainly due to the presence of high series resistance ( $R_s$ ) of the diode. So, in this work, we have also measured the  $R_s$  of the device. To measure  $R_s$ , we have used the Cheng Cheung equation given below [22-26],

$$\frac{dV}{d \ln I} = \frac{nKT}{q} + IR_s \tag{9}$$

$$H(I) = n\phi_b + IR_s \tag{10}$$

Where,

$$H(I) = V - \left( \frac{nKT}{q} \right) \ln \frac{I}{AA^*T^2} \tag{11}$$

From Eq. (9), we have measured the device  $R_s$ . To extract the device  $R_s$ , we have plotted  $\frac{dV}{d \ln I}$  Vs. I curve shown in Fig.11a. The  $\frac{dV}{d \ln I}$  vs. I plot gives a straight line with an intercept of  $\frac{nKT}{q}$ . We have extracted the value of  $\eta$ , and the curve's slope gives the value of  $R_s$  from the intercept. We have also measured the value of  $R_s$  by using Eq. (10). According to the equation, we have plotted H (I) vs. I curve shown in Fig. 11b. We have extracted the value of  $R_s$  from the slope from this curve, and the intercept gives the value of barrier height ( $\phi_b$ ). The extracted values of  $R_s$  of the turmeric dye-based diode by using  $\frac{dV}{d \ln I}$  vs. I and H (I) vs. I plot shows consistency with each other. The extracted values are shown in Table 2.

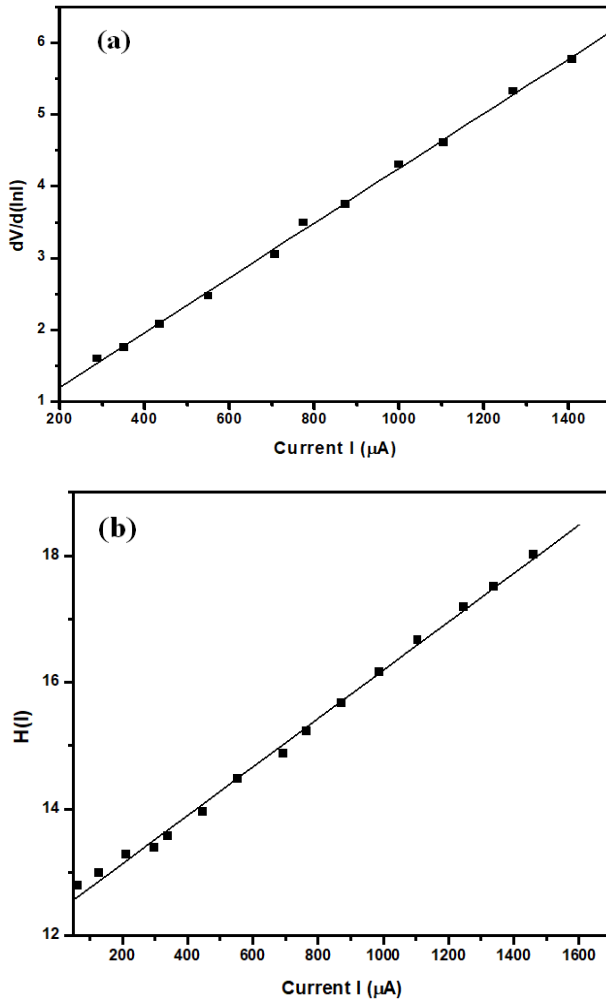


Fig. 11. (a)  $dV/d\ln I$  - Current ( $I$ ) and (b)  $H(I)$  – Current ( $I$ ) plot of turmeric dye-based herbal diode.

Table 2. Extracted values of  $n$ ,  $\phi_b$ , and  $R_s$  of the turmeric dye-based herbal diode.

Sample	Value of $n$	Value of $\phi_b$	$R_s$ from $dV/d\ln I$ plot ( $K\Omega$ )	$R_s$ from $H(I)$ vs $I$ plot ( $K\Omega$ )
ITO/turmeric/Al	16.73	0.74	3.82	3.81

The above result shows that the turmeric dye gives a good response as an herbal diode. The value of  $n$  of the turmeric diode is nearly about 16.73, and the value of  $R_s$  is 3.81  $K\Omega$ . The value of  $R_s$  was measured by the Cheung Cheng method and verified the value by using the  $H(I)$  vs.  $I$  plot. The extracted value of  $R_s$  by using these two methods is nearly similar to each other that exhibits the consistency of these two methods. It is observed that the electronics parameters  $n$  and  $R_s$  are high of the turmeric dye-based diode. There are

several reasons for this high value of ideality factors such as interfacial properties of the metal herbal dye contact, irregularities in the thickness of herbal dye, charge recombination process, and the presence of series resistance.

It is well known that in any semiconductor-based electronic and optoelectronic device, the contact resistance and the neutral region of the semiconductor contribute to the device  $R_s$ . Now in the case of herbal semiconductors, they do not have a clearly defined band structure. The energy band is defined by HOMO and LUMO where HOMO is the highest occupied molecular orbital and LUMO stands for lowest unoccupied molecular orbital. Due to this structural disorder and the weak molecular bonding, these herbal dyes are prone to have electronic traps which introduce additional energy levels inside the energy band between HOMO and LUMO. The trap state restricted the charge carrier's flow at the interface throughout the structure, and due to this, the overall current of the turmeric dye-based herbal diode is reduced. So, in this work, we have also measured the trapped energy of the device. To measure the trapped energy, we have considered the distribution of traps as exponential, and by using this distribution, the trapped energy concentration can be given by [27],

$$n_t = H_n \exp\left(\frac{F_n}{KT_c}\right) \quad (12)$$

Where  $H_n$  is the trap density,  $F_n$  is the electron Fermi level,  $K$  is the Boltzmann constant, and  $T_c$  is the characteristic temperature which is given by,

$$T_c = \frac{E_c}{K} \quad (13)$$

Where  $E_c$  is the characteristic trap energy.

Now by this considering this exponential trap distribution, we have estimated the  $E_c$  from the space charge limited current given by,

$$I = AN_c\mu Q^{1-m} \left(\frac{m\varepsilon}{H_n(m+1)}\right)^m \left(\frac{2m+1}{m+1}\right)^{m+1} \left(\frac{V^{m+1}}{L^{2m+1}}\right) \quad (14)$$

Where  $N_c$  is the effective density of states,  $\mu$  is the mobility,  $\varepsilon$  is the product of the permittivity of the vacuum ( $\varepsilon_0$ ) and the dielectric constant ( $\varepsilon_r$ ),  $V$  is the applied voltage,  $L$  is the thickness of the active layer, and  $m$  is the ratio of the characteristic temperature  $T_c$  with absolute temperature  $T$  ( $m = \frac{T_c}{T}$ ).

From Eq. (14), it can be said that the space charge limited current exhibits the power-law dependence in between current voltage,

$$I \approx V^{m+1} \quad (15)$$

Using this equation, we have estimated the trapped energy of the herbal diode from  $\ln I$  vs.  $\ln V$  plot. The  $\ln I - \ln V$  plot has shown in Fig. 12.

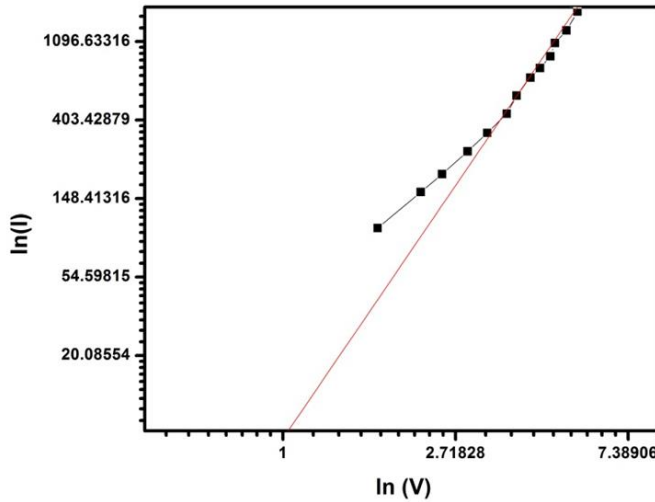


Fig. 12. lnI - lnV plot of turmeric dye-based herbal device.

From Fig. 12 it can be observed that the plot has two regions. One region is below transition voltage, where the value of  $m$  is less than 1. In this region, the conduction process is governed by ohmic conduction. While the others one is at the above transition voltage where SCLC governs the conduction process. In this region, the value of  $m$  is greater than 2. The extracted values of  $m$  and  $E_c$  have given in Table 3.

Table 3. Extracted values of  $m$  and  $E_c$  of the turmeric dye-based herbal diode.

Sample	Value of $m$	Value of $E_c$ (eV)
ITO/turmeric/Al	2.3	0.059

From the above result, it can be concluded that as the herbal dye prone to have traps, the charge injection and transport mechanism get restricted. So due to this, the overall device's current gets reduced, and the electronic parameters  $n$ ,  $R_s$  of the diode are high compared to semiconductor diode. From the above result, it can also be said that by reducing the trapped energy of the herbal diode, we can enhance the device current and improve the diode's different electronic parameters.

**Conclusion**

In this work, we have studied the charge carrier density of PVA turmeric composite thin film. The extracted value is about  $2.8 \times 10^{23} \text{ m}^{-3}$ . This result is quite satisfactory in comparison with inorganic substances. We have also calculated the mobility of the charge carrier ( $\mu$ ), which is a product of the Hall coefficient and conductivity of the film. The value of Hall mobility is  $3.3 \times 10^{-13} \text{ m}^2 \text{ volt}^{-1} \text{ sec}^{-1}$ . Though mobility and conductivity of turmeric dye thin film are low, the charge carrier density is quite high. From this result, it may be said that the turmeric dye will be a good candidate for the preparation of the

herbal device. In addition, we have prepared one turmeric dye-based herbal diode and studied various electronic parameters, such as reverse saturation current, rectification ratio, ideality factor, series resistance, and barrier height. It is observed that the extracted values of ideality factor and series resistance are very high, which are about 16.73 and 3.82 K $\Omega$ , respectively. One of the main reasons for these high values is the presence of traps in turmeric dye. The computed value of trap energy of the device is about 0.059 eV. The presence of traps restricted the charge transport through the device, and it can conclude that by lowering the trapped energy, we can improve the overall performance of the device.

### Acknowledgment

The authors would like to thank RUSA, West Bengal, who gave financial support to do the research work. We are grateful to A. N. Basu, Department of Physics, Jadavpur University, for providing us valuable suggestions throughout this work.

### References

1. A. M. Deberao, P. P. Kolte, and R. N. Turukmane, *Int. J. Res. Sci. Innovat. (IJRSI)* **3** (2016).
2. H. Krizova, *Natural dyes: Their Past, Present, Future and Sustainability*. In *Recent Developments in Fibrous Material Science*, ed. D. Křemenáková et al. (Kanina: Prague, Czech Republic, 2015) pp. 59-71.
3. K. E. Jasim, S. Cassidy, F. Z. henari, and A. A. Dakhel, *J. Energy Power Eng.* **11**, 409 (2017). <https://doi.org/10.17265/1934-8975/2017.06.006>
4. S. Shalini, R. B. Prabhu, S. Prasanna, T. K. Mallick, and S. Senthilarasu, *Renewable Sustainable Energy Rev.* **51**, 1306 (2015). <https://doi.org/10.1016/j.rser.2015.07.052>
5. G. Richhariya, A. Kumar, P. Tekasakul, and B. Gupta, *Renewable Sustainable Energy Rev.* **69**, 705 (2017). <https://doi.org/10.1016/j.rser.2016.11.198>
6. K. Feron, W. J. Belcher, C. J. Fell, and P. C. Dastoor, *Int. J. Mol.* **13**, 17019 (2012). <https://doi.org/10.3390/ijms131217019>
7. S. Sen and N. B. Manik, *Int. J. Sci. Res. Rev.* **7**, (2019).
8. P. K. Das, S. Bhunia, and N. B. Manik, 9781003055174 (Apple Academic Press, 2020).
9. P. K. Das, S. Bhunia, and N. B. Manik, *Adv. Mater. Res.* **1159**, 112 (2020). <https://doi.org/10.4028/www.scientific.net/AMR.1159.112>
10. T. I. Benanti and D. Venkataramaan, *Photosynth. Res.* **87**, 73 (2006). <https://doi.org/10.1007/s11120-005-6397-9>
11. N. A. N. Aziz, M. I. N. Isa, and S. Hasiah, *J. Clean Energy Technol.* **2**(4), 322 (2014). <https://doi.org/10.7763/JOCET.2014.V2.148>
12. V. Vohra, *Materials* **11**, 2579 (2018). <https://doi.org/10.3390/ma11122579>
13. A. A. Huaman, M. R. Celestino, and M. E. Quintana, *Royal Soc. Chem.* **11**, 9086 (2021). <https://doi.org/10.1039/D1RA01043C>
14. A. R. N. Laily, H. Salleh, N. A. N. Aziz, A. N. Dagang, and S. M. Ghazali, *Mater. Sci. Energy* **846**, 264 (2018), <https://doi.org/10.4028/www.scientific.net/MSF.846.264>
15. S. Hasiah, K. Ibrahim, H. B. Senin, and K. B. K. Halim, *J. Phys. Sci.* **19**, 77 (2008). <https://doi.org/10.1063/1.3160184>
16. S. Ilić, V. P. Series: *Electronics and Energetics* **32**, 91 (2019). <https://doi.org/10.2298/FUEE1901091I>
17. C. Kittel, *Introduction to Solid State Physics*, 4<sup>th</sup> Edition (J. Wiley and Sons Inc, N. Y., 1971).

18. S. Sen and N. B. Manik, Int. J. Adv. Sci. Eng. **6**, 23 (2020).  
<https://doi.org/10.29294/IJASE.6.S2.2020.23-27>
19. S. Bhunia, P. K. Das, and N. B. Manik, J. Ind. Chem. Soc. **97** (2020).
20. P. K. Das, S. Sen, and N. B. Manik, Ind. J. Phys. (2021). <https://doi.org/10.1007/s12648-021-02051-y>
21. S. Chakraborty and N. B. Manik, Front. Optoelectronics **8**, 289 (2015).  
<https://doi.org/10.1007/s12200-015-0527-6>
22. P. K. Das and N. B. Manik, Int. J. Renewable Energy Technol. (IJRET) **12**, 118 (2021).  
<https://doi.org/10.1504/IJRET.2021.115280>
23. M. Shah, M. H. Sayyad, K. S. Karimov, and F. Wahab, J. Appl. Phys. **43**, ID 405104 (2010).  
<https://doi.org/10.1088/0022-3727/43/40/405104>
24. F. Yakuphanoglu, Synth. Met. **160**, 1551 (2010).  
<https://doi.org/10.1016/j.synthmet.2010.05.024>
25. S. K. Cheung and N. W. Cheung, Appl. Phys. Lett. **49**, 85 (1986).  
<https://doi.org/10.1063/1.97359>
26. M. Benhaliliba, J. Nano-Electron. Phys. **7**, ID 02029 (2015).
27. G. Kunakova, R. Viter, S. Abay, S. Biswas, J. D. Holmes, T. Bauch, F. Lombardi, and D. Erts, J. Appl. Phys. **119**, ID 114308 (2016). <https://doi.org/10.1063/1.4944432>